Journal of Controlled Release 197 (2015) 208–218

Contents lists available at ScienceDirect

Journal of Controlled Release

journal homepage: www.elsevier.com/locate/jconrel

Simultaneous delivery of therapeutic antagomirs with paclitaxel for the management of metastatic tumors by a pH-responsive anti-microbial peptide-mediated liposomal delivery system

Qianyu Zhang, Rui Ran, Li Zhang, Yayuan Liu, Ling Mei, Zhirong Zhang, Huile Gao, Qin He *

Key Laboratory of Drug Targeting and Drug Delivery Systems, West China School of Pharmacy, and State Key Laboratory of Biotherapy/Collaborative Innovation Center of Biotherapy, West China Hospital, Sichuan University, Chengdu, 610041, China

ARTICLE INFO

Article history:
Received 23 May 2014
Accepted 10 November 2014
Available online 15 November 2014

Keywords:
anti-microbial peptides
[D]-H_6L_9
Liposomes
Antagomir-10b
Co-delivery
Metastasis

ABSTRACT

The roles of microRNAs (miRNAs) in the regulation of metastasis have been widely recognized in the recent years. Mir-10b antagomir (antagomir-10b) was shown to impede metastasis through the down-regulation of mir-10b; however, it could not stunt the growth of primary tumors. In this study we showed that the co-delivery of antagomir-10b with paclitaxel (PTX) by a novel liposomal delivery system modified with an anti-microbial peptide [D]-H_6L_9 (D-Lip) could significantly both hinder the migration of 4 T1 cells and induce evident cellular apoptosis and cell death in the meantime. The histidines in the sequence of [D]-H_6L_9 allowed the peptide to get protonated under pH 5.0 (mimicking the lysosome/endosome environment), and strong membrane lytic effect could thus be activated, leading to the escape of liposomes from the lysosomes and the decrease of of mir-10b expression. The in vivo and ex vivo fluorescence imaging showed that D-Lip could reach 4 T1 tumors efficaciously. Incorporation of PTX did not influence the antagomir-10b delivery effect of D-Lip; for the in vivo tumor inhibition assay, compared with all the other groups, the combination of antagomir-10b and PTX delivered by D-Lip could prominently delay the growth of 4 T1 tumors and reduce the lung metastases at the same time, and the expression of Hoxd10 in tumors was also significantly up-regulated. Taken together, these results demonstrated that D-Lip could act as a sufficient tool in co-delivering antagomir-10b and PTX.

1. Introduction

MicroRNAs (miRNAs) are a class of non-coding RNAs operating mainly on post-transcriptional gene silencing, and are responsible for the modulation of cell growth, proliferation, differentiation, motility and apoptosis [1]. Therefore, miRNAs received substantive attention and have been broadly investigated as a novel class of RNA therapeutics for cancer [2–4]. Metastasis of cancer has been considered as a major process in cancer progression, and several miRNAs have been identified to be involved in the metastatic progression process [5,6]. MicroRNA-10b (mir-10b), as discovered by Ma et al. [7], could initiate the tumor invasion and metastasis in breast cancer. Mir-10b was up-regulated in metastatic breast cancer cells rather than non-metastatic cells [7], and inhibition of Mir-10b could result in decreased incidence of metastases of tumor cells [8].

For the inhibition of corresponding miRNAs, antagomirs (also known as anti-miRs) have emerged as a kind of single-stranded RNA analogues with chemical modification and cholesterol conjugation to guarantee their stability [9], and functioned by hybridizing and repressing the activity of a mature miRNA [10]. Ma et al. have silenced Mir-10b with antagomir-10b in a murine breast cancer metastatic cancer, and found that metastases of tumors could be significantly reduced [11]. However, high dose of antagomir-10b (as much as 50 mg/kg) was required for a sufficient inhibition over tumor metastasis [11]. Although the toxicity was minimal according to the researcher, due to the nature of antagomirs, extensive distribution of free antagomir-10b *in vivo* could still cause slight abnormity on liver and spleen size and levels of several serum proteins and metabolites [11]. And also, as antagomir-10b was reported to show little influence on tumor cell growth and viability [8,11], how to impede the growth of primary tumor seemed to be a tricky problem. In this sense, drug delivery systems loaded with both metastasis-inhibitor antagomir-10b and another cytotoxic reagent that could lead to increased accumulation in tumor and reduced accumulation in non-targeted organs were highly desirable. Liposome-based drug delivery system has earned notable renown over the past years [12]. Due to the excellent delivery capacities of liposomes, the co-delivery of genes as well as cytotoxic reagents (such as doxorubicin and paclitaxel) by liposomal delivery system has been adopted to achieve combined or synergistic effect [13–15]. Thus it was envisaged that the co-delivery of antagomir-10b would be feasible when mediated by liposomes.

Successful cytoplasmic delivery of genes (endosome/lysosome escape) after the internalization of vectors ensured the efficiency of gene

* Corresponding author. Tel./fax: +86 28 85502532.
E-mail address: qinhe@scu.edu.cn (Q. He).

http://dx.doi.org/10.1016/j.jconrel.2014.11.010
0168-3659/

delivery, as the pH could drop to 5.5–6.0 in endosomes and 4.5–5.0 in lysosomes [16], leading to degradation of genes and resulting in low transfection efficacy. Many researchers have concentrated on this phenomenon, and have "turned waste into wealth", which means utilizing the acidification of endosome and lysosome environment to fabricate pH-responsive gene carriers [17–19]. Histidine, with a pK_a around 6.5 [20], came to people's attention as it could remain slightly negatively charged under physiological condition and protonate into positive charge in acidic environment, and histidine-rich cell penetrating peptides and drug delivery system mediated by them have been explored accordingly [21–24]. Other than cell penetrating peptides, antimicrobial peptides (AMPs, also known as host defense peptides) containing histidines have also come into view for tumor delivery [25–27]. These peptides were designed by replacing the lysines in the peptide sequence into histidine, thus neutralizing their charge under pH 7.4, and hopefully their activity could only be set off in environment with lowered pH. Most of the cases, these peptides were directly applied to tumor cells for cell lysis and tumor inhibition [25–27], showing high membranelytic activity under acidified environment. Antimicrobial peptides have also been used to deliver different cargoes for cancer treatment [28]. However, very few of them have been discussed as the possible candidates of mediating drug delivery vehicles. We made a bold assumption that drug delivery system modified with histidine-rich antimicrobial peptides could yield considerable transfection efficiency. In this work, we utilized peptide [D]-H_6L_9, a pH-dependent antimicrobial peptide reported by Makovitzki et al. [27], and tethered it onto the surface of liposomes (Fig. 1). Liposome was consequently loaded with antagomir-10b (metastasis inhibitor) and paclitaxel (PTX, cytotoxic reagent) for the treatment of murine metastatic mammary tumor models.

2. Materials and methods

2.1. Materials

[D]-H_6L_9 peptide with a terminal cysteine (LHLLHHLLHHLLHLL-Cys, the underlined letters were D-amino acids) was synthesized according to the standard solid phase peptide synthesis by ChinaPeptides Co. Ltd. (Shanghai, China). Antagomir-10b and Cy5-labeled antagomir-10b were ordered from RiboBio (Guangzhou,China) as ready-made products, and the sequence of antagomir-10b was complementary to the mature mmu-mir-10b-5p, which was as following: 5′-CACAAAUU CGGUUCUACAGGGUA-Chol-3′, in which all the nucleotides were all 2′-O-Me-modified. Cholesterol was linked onto the 3′ end, and phosphorothioate linkage modification was performed on both the 5′ end and 3′ end. Bulge-loop ™ miRNA qRT-PCR primer sets for Mir-10b and U6 small nuclear RNA were purchased from RiboBio (Guangzhou, China). FITC-conjugated Hoxd10 antibody was purchased from Biorbyt Ltd. (Cambridge, UK). Soybean phosphatidylcholine (SPC) was purchased from Shanghai Taiwei Chemical Company. DSPE-PEG_{2000} and DSPE-PEG_{2000}-Mal were purchased from Avanti Polar Lipids (Alabaster, AL, USA).1,2-dioleoyl-3-trimethylammonium-propane (DOTAP) was obtained from Shanghai Advanced Vehicle Technology (AVT) L.T.D.

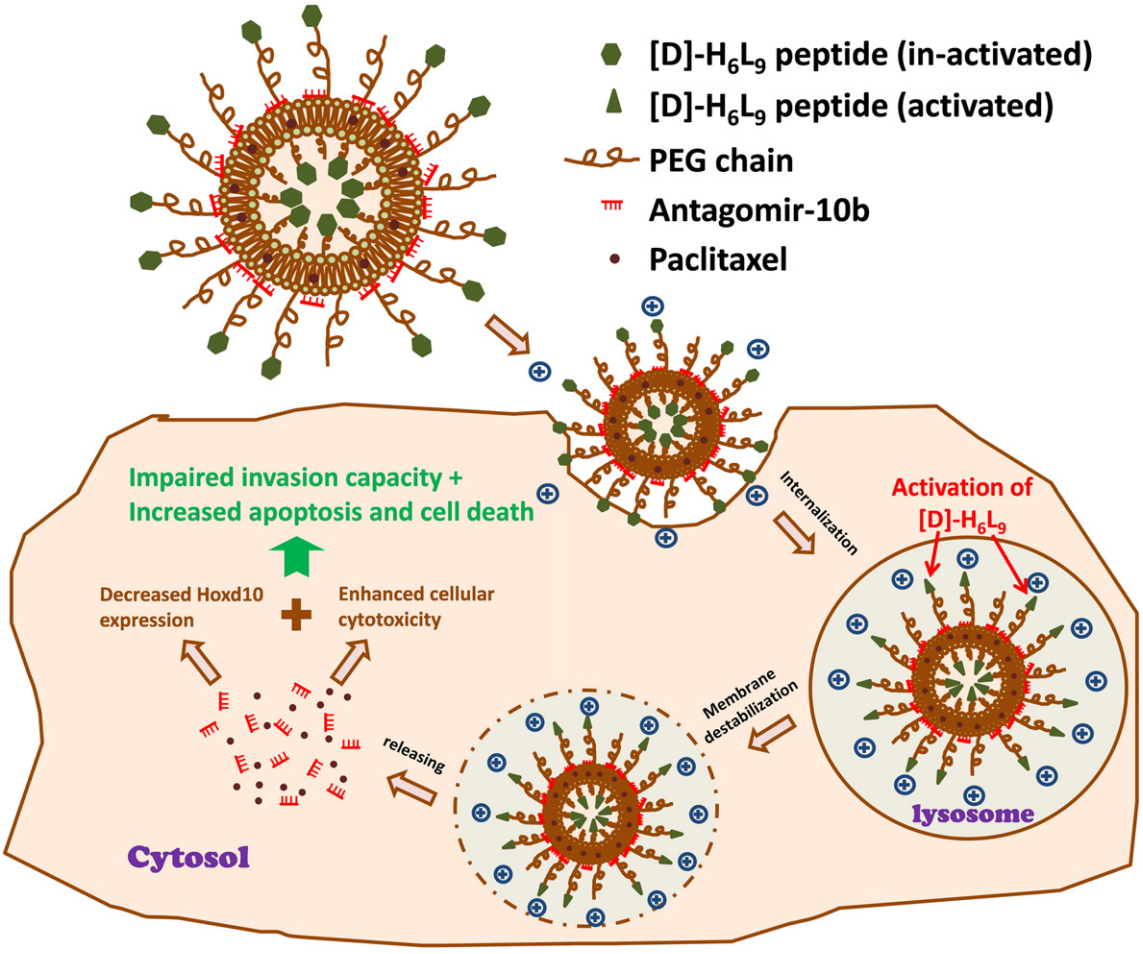

Fig. 1. Schematic illustration of the intracellular fate of D-Lip co-delivering antagomir-10b and PTX. Upon internalization into the cells and got integrated into the lysosomes, the zeta potential of antagomir-10b and PTX co-loaded D-Lip increased due to the histidines in the peptide sequence of [D]-H_6L_9, and the membrane-lytic activity of [D]-H_6L_9 modified on the liposomes was also activated under the acidified compartment, triggering strong membrane-destabilization effect. Antagomir-10b and paclitaxel could be successfully released into the cytosol and impair the cellular invasion capacity as well as mediate strong cellular apoptosis and cell death.

Company (Shanghai, China). Amiloride, chlorpromazine and genistein were obtained from Sigma-aldrich ((St. Louis, MO, USA). 40, 6-diamidino-2-pheylindole (DAPI) and Triton X-100 were purchased from Beyotime Institute Biotechnology (Haimen, China). Lipofectamine 2000 was obtained from Life Technologies (Carlsbad, CA, USA). Lysotracker™ green was purchased from Invitrogen (Carlsbad, CA, USA). 1, 10- Dioctadecyl- 3, 3, 3, 3 – tetramethyl indotricarbocyanine iodide (DiR) was purchased from Biotium (Hayward, CA, USA). Plastic cell culture dishes and plates were purchased from Wuxi NEST Biotechnology Co. (Wuxi, China).Other chemicals and reagents were of analytical grade.

2.2. Cell lines and tumor models

4 T1 cells (murine breast cancer cells) were cultured in RPMI-1640 medium (GIBCO) supplemented with 10% FBS at 37 °C in a humidified 5% CO_2 atmosphere.

BALB/c mice were purchased from experiment animal center of Sichuan University (P.R. China). All animal experiments were performed in accordance with the principles of care and use of laboratory animals and were approved by the experimental animal administrative committee of Sichuan University. For the establishment of tumor models, 1×10^6 4 T1 cells were orthotopically implanted into the mammary fat pad of 8-week old female BALB/c mice. Primary tumor growth was calculated from caliper measurements with the following formula, $(L \times W^2)/2$ (L, length; W, width) [29].

2.3. Synthesis of DSPE-PEG_{2000}-[D]-H_6L_9

DSPE-PEG_{2000}-Mal (1 eq) was dissolved in chloroform, and then Cys-[D]-H_6L_9 (1.2 eq) dissolved in methanol was added into the DSPE-PEG_{2000}-Mal solution. The above mixed solution was allowed to react in the presence of nitrogen for about 48 h in darkness under room temperature. After thin layer chromatography confirmed the disappearance of DSPE-PEG_{2000}-Mal, the organic solvent was filtered and the filtrate was evaporated by rotary evaporation. The residue was redissolved by chloroform and filtered again for purification. The supernatant was evaporated by rotary evaporation and stored under -20 °C until used.

2.4. Preparation and characterization of liposomes

Liposomes were prepared by the thin film hydration method. SPC, DOTAP, DSPE-PEG_{2000} and DSPE-PEG_{2000}-[D]-H_6L_9 (molar ratio = 45: 45: 2: 8) were dissolved in the mixture of chloroform and methanol (v/v = 4:1). Then the organic solvent was removed by rotary evaporation, and the film was further dried and stored in vacuum overnight. The thin film was hydrated in DEPC-treated water under 37 °C for 30 min. Then it was further intermittently sonicated by a probe sonicator at 80 W for 100 s to form the [D]-H_6L_9 modified cationic liposome (D-Lip). PEGylated cationic liposome (PEG-Lip) was prepared with SPC, DOTAP and DSPE-PEG_{2000} (molar ratio = 45: 45: 10). PTX-loaded liposomes were prepared with PTX added to the lipid organic solution prior to the solvent evaporation. The entrapment efficiency (EE%) of PTX was determined by HPLC. The EE% of antagomir-10b was determined after loading liposomes with Cy5-labeled antagomir-10b. Liposomes were pipetted into ultra-filtration tubes (30 K, Pall Corporation, Michigan, USA), and centrifuged at 4000 rpm for 30 min. Liposomes and filtered solution were both lysed with 1% triton X-100 and measured by a microplate reader (Thermo Scientific Varioskan Flash) with an excitation wavelength of 570 nm and emission wavelength of 630 nm. Lipofectamine incubated with antagomir-10b (Lipofectamine/Antagomir-10b) was prepared by incubating Lipofectamine 2000 with antagomir-10b for 15 min under room temperature and was considered as the positive control in some in vitro assays. Appropriate amount of DiR were also added to the solution before the solvent evaporation to prepare DiR-loaded liposomes.

Liposomes were all sterilized by passing through 0.22 μm sterile filter. For the liposomes loaded with antagomir-10b, 0.5 mL liposomes (containing 2 μmol lipids) was incubated with 6 nmol antagomir-10b or Cy5-labeled antagomir-10b in darkness under room temperature for 30 min. This loading procedure was performed immediately before use.

The morphology of D-Lip was observed under transmission electronic microscope (TEM) (JEM 100CX, JEOL, Japan). The hydrodynamic diameters and zeta potentials of the D-Lip and PEG-Lip were measured by Malvern Zetasizer Nano ZS90 instrument (Malvern instruments Ltd. U. K.).

2.5. Turbidity variation in serum

Turbidity variations of liposomes incubated with fetal bovine serum (FBS) were monitored. Briefly, liposomes were mixed with equal volume of FBS under 37 °C with gentle shaking. At each pre-set time points, 200 μl of the sample was pipetted out and onto a 96-well plate to measure the transmittance at 750 nm by a microplate reader (Thermo Scientific Varioskan Flash).

2.6. Hemolysis assay

For the hemolysis study, fresh rat blood was collected, and red blood cells (RBCs) were obtained after centrifugation and washed with PBS. The RBC suspension (2%, v/v) was mixed with liposomes under different pH conditions at 37 °C for 2 h, 4 h and 6 h respectively. After the incubation, the supernatant was separated after centrifugation and subjected to measurement for hemoglobin release by microplate reader (Thermo Scientific Varioskan Flash) at 545 nm. Samples incubated with 1% Triton X-100 served as the positive control (100% hemolysis) and samples incubated with PBS as the negative control (0% hemolysis) respectively. The degree of hemolysis was calculated by the following equation:

$$\text{Hemolysis}(\%) = (A\text{-}A_{0\%})/(A_{100\%}\text{-}A_{0\%})$$

Where A, $A_{0\%}$ and $A_{100\%}$ represented the absorbance of samples incubated with liposomes, samples with 100% hemolysis and samples with 0% hemolysis respectively.

2.7. MTT assay and in vitro cellular apoptosis assay

4 T1 cells were seeded onto a 96-well plate at a density of 2×10^3 cells/well. After 24 h the cell culture media was replaced with liposome-containing culture medium and the incubation continued for another 48 h. By the end of the incubation, 20 μL MTT solution (5 mg/mL in PBS) was added into each well and cells were further incubated for 4 h under 37 °C. Then the media was removed and cells were dissolved by 150 μL dimethyl sulfoxide. The absorbance was measured by a microplate reader (Thermo Scientific Varioskan Flash) at 490 nm.

The analysis of apoptosis induced by different preparations was determined after annexin V-FITC/PI double staining according to the manufacturer's protocols (Annexin V-FITC Apoptosis Detection Kit, KeyGen biotech, China). Briefly, by the end of the treatment, cells were harvested, washed with cold PBS, suspended in 500 μL binding buffer and stained by 5 μL Annexin V-FITC and 5 μL PI. The cells were incubated in the dark for 15 minutes and then measured by flow cytometer (Cytomics™ FC 500, Beckman Coulter, Miami, FL, USA).

2.8. Wound-healing assay

2×10^5 cells/well of 4 T1 cells were planted onto 12-well plate and were allowed to grow to achieve 90% confluence as a monolayer. A vertical wound was scratched with a 200 μL pipette tip. Wounded cells were gently washed PBS for 3 times to remove the detached cells, and fresh medium without serum containing liposomes was replenished

and cells were cultured for an additional 48 h. Cells were observed and photographed under Carl Zeiss 40CFL Axiovert 40 inverted microscope (Germany).

2.9. Cellular uptake of liposomes and the subcellular localization

For cells analyzed by cytometry, 4 T1 cells were seeded onto 6-well plate at a density of 5×10^5 cells/well and allowed for attachment overnight. Cy5-labeled antagomir-10b-loaded liposomes were then added to each well, and the incubation lasted for another 2 h. Cells were washed with cold PBS for three times, and were trypsinized and resuspended in 0.4 mL PBS. The fluorescent intensity of cells was measured by a flow cytometer (Cytomics™ FC 500, Beckman Coulter, Miami, FL, USA) with the excitation wavelength at 630 nm and the emission wavelength at 680 nm. The evaluation of different inhibitors on the cellular uptake was performed as previously described [24]. Ten thousand events were recorded for each sample.

For cells observed by confocal laser scanning microscopy, 1×10^5 cells/well of 4 T1 cells were seeded on gelatin coated cover slip in a six-well plate. After 2 h of incubation with Cy5-labeled antagomir-10b loaded liposomes, cells were washed with cold PBS for three times and fixed with 4% paraformaldehyde at room temperature for 15 min, following by nuclei staining with DAPI for 5 min. As for cells for subcellular localization assay, at the end of incubation with Cy5-labeled antagomir-10b-loaded liposomes, lyso-tracker green was applied to each well (200 nM) and incubated for 30 min. After washing with cold PBS for 3 times, cells were fixed with 4% paraformaldehyde at room temperature and stained with DAPI, and then was subjected to observation under confocal microscope (FV1000, Olympus, USA).

2.10. In vitro evaluation on the effect of antagomir-10b loaded liposomes on mir-10b silencing and Hoxd10 expression

2.10.1. In vitro quantification of mir-10b

4 T1 cells were firstly incubated with different antagomir-10b-loaded preparations for 48 hours. Then total RNA in cells were isolated with miRcute miRNA Isolation kit (Tiangen biotech, Beijing, China), and were transcribed into cDNA with the sequence-specific stem-loop RT primers for mir-10b according to the manufacturer's instructions (RiboBio, Guangzhou, China). Quantitative PCR was then performed using Ssofast™ Evagreen® Supermixkit (Bio-rad, CA, USA) in triplicates. Data were normalized to an internal control U6 small nuclear RNA and were analyzed with the iQ™5 Real Time PCR detection system (Bio-rad, CA, USA).

2.10.2. In vitro Hoxd10 nuclear protein staining

For cells observed by confocal laser scanning microscopy, 1×10^5 cells/well of 4 T1 cells were seeded on gelatin coated cover slip in a six-well plate. Antagomir-10b loaded liposomes were then added to each well, and the incubation lasted for another 48 h. Cells were washed with cold PBS for three times, and were trypsinized and resuspended in 4% paraformaldehyde at room temperature for fixation. Then cells were treated with 0.1% Triton X-100 for 20 min for permeation. Cells were later washed and collected and blocked in 1% BSA for 120 min, and FITC-conjugated Hoxd10 antibody was applied in 1% BSA for intracellular staining for 30 min. Cells were then observed by confocal microscope through the FITC fluorescence channel (FV1000, Olympus, USA).

2.11. In vivo bio-distribution study

Bio-distribution study was carried out when volumes of the 4 T1 tumors reached around 50 mm^3. Mice were injected with free Cy5-labeled antagomir-10b or Cy5-labeled antagomir-10b-loaded liposomes. Twenty-four hours later, mice were imaged with IVI® Spectrum system (Caliper, Hopkington, MA, USA), and immediately executed with cervical dislocation. Hearts, livers, spleens, lungs, kidneys and tumors were collected. All the organs were imaged with IVI® Spectrum system (Caliper, Hopkington, MA).

2.12. In vivo therapeutic experiment

Treatment started on the 5th day of tumor inoculation, and mice were assigned into 6 groups ($n = 6$) and administered with the following six preparations respectively: PBS, Free antagomir-10b, PEG-Lip/Antagomir-10b (PEG-Lip loaded with antagomir-10b), D-Lip/Antagomir-10b (D-Lip loaded with antagomir-10b), D-Lip/Antagomir-10b + PTX (D-Lip co-loaded with antagomir-10b and PTX) and D-Lip/PTX (D-Lip loaded with PTX). All the preparations were injected through tail veins every 3 days for 6 times, and tumor volumes and animal body weights were monitored. Antagomir-10b was administered at a dose of 2 mg/kg, and PTX was administered at a dose of 2 mg/kg. On the 28th day mice were sacrificed, and lungs and tumors were collected. The expression of Hoxd10 protein in tumors was measured with mouse Hoxd10 Elisa kit (Cusabio, Wuhan, China). Ki67 and TUNEL staining of the paraffin-embedded tumors were performed according to the standard protocols provided by the manufacturers.

2.13. Statistical analysis

Statistical comparisons were based on Student t-test, and p value < 0.05 and <0.01 were considered indications of statistical difference and statistically significant difference respectively.

3. Results and discussions

3.1. Characterization of liposomes

The successful synthesis of DSPE-PEG_{2000}-[D]-H_6L_9 was confirmed by mass spectrometry (as shown in Fig. S1). The observed molecular weight of the final product was 4908 Da, which was close to the theoretical molecular weight of 4903 Da. D-Lip exhibited uniform and spherical appearance under TEM observation (Fig. S2). Particle sizes and zeta potentials of liposomes were measured (Table 1). It could be seen that D-Lip underwent drastic zeta potential variation under different pH conditions. The zeta potential went from 20.6 ± 1.2 mV under pH 7.4 (very close to PEG-Lip) to 38.9 ± 2.1 mV under pH 5.0 (mimicking endosome/lysosome environment, from ref. [30]), while there was no significant change in sizes. By comparison, there was no obvious change in both zeta potentials and sizes under different pH conditions for PEG-Lip. Characteristics of liposomes could be greatly influenced by its surface modification of pH-responsive peptide as we have reported before [24]. The variation of zeta potentials of D-Lip was attributed to the existence of histidines in [D]-H_6L_9, and it could respond quickly to different pH conditions. From the results it could be concluded that D-Lip has been imparted with a rather high positive charge under pH 5.0 (48.9 ± 2.1 mV), and membrane lytic activity of [D]-H_6L_9 might be activated in this endosome/lysosome-mimicking environment.

3.2. Turbidity variation and hemolysis of liposomes

As displayed in (Fig. 2), there was no obvious change in the serum turbidity for D-Lip as well as PEG-Lip, meaning that no aggregation of liposomes was formed, emphasizing their stability in serum which was

Table 1
The particle sizes and zeta potentials of D-Lip and PEG-Lip under different pH.

	Size(nm)	PDI	Zeta potential(mV)
D-Lip(pH 7.4)	145.2 ± 4.3	0.257 ± 0.072	20.6 ± 1.2
D-Lip(pH 5.0)	139.2 ± 9.1	0.215 ± 0.087	38.9 ± 2.1
PEG-Lip(pH 7.4)	130.2 ± 8.9	0.199 ± 0.062	19.9 ± 7.2
PEG-Lip(pH 5.0)	126.1 ± 1.9	0.221 ± 0.033	17.9 ± 8.3

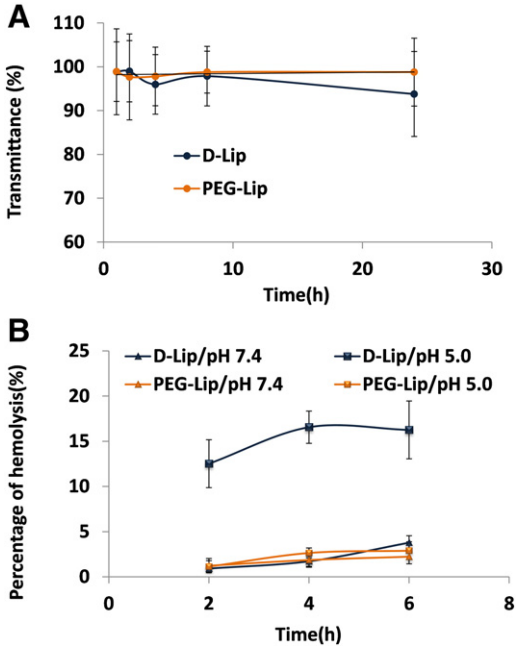

Fig. 2. (A) The turbidity variation (represented by transmittance) of PEG-Lip and D-Lip in 50% FBS. (B) Hemolytic activity of PEG-Lip and D-Lip on red blood cells under pH 7.4 and pH 5.0. (n = 3, mean ± SD).

mainly due to the PEG corona on the liposome surface. As for the hemolysis property of liposomes under different pH conditions, surprisingly we found that under pH 5.0, the percentages of hemolysis of D-Lip were 12.5 ± 2.6% at 2 h, 16.6 ± 1.8% at 4 h and 16.2 ± 3.2% at 6 h respectively; on the contrary, the hemolytic ratio of D-Lip under pH 7.4 and PEG-Lip under both pH 7.4 and pH 5.0 all remained below 4% at each time point. Hemolytic activity of NPs on RBCs has been regarded as an indication to evaluate the ability of NPs to rupture endolysosomes [30,31]. This pH-dependent membrane-lytic activity was clearly brought by [D]-H_6L_9. Combined with results from zeta potential measurement, it could be pointed out that under pH 5.0, the zeta potential of D-Lip was remarkably elevated, and the membrane-disruptive nature of [D]-H_6L_9 was triggered. [D]-H_6L_9 was derived from [D]-K_6L_9, which can cause cancer cell lysis when injected intratumorally [32]. The replacement of lysines with histidines would decrease the net positive charge of the original peptide [D]-K_6L_9. The electrostatic attraction between negatively charged components of cells and the positively charged peptides played a major role in its ability to disrupt the membrane of cells [33], thus the comparatively decreased net charge of [D]-H_6L_9 could result in decreased cell lytic activity under normal pH and increased cell permeation in acid environment. Makovitzki [27] mentioned that under pH 6.0, [D]-H_6L_9 could induce more calcein leakage compared with pH 7.4, all because the membrane-lytic activity was restored under acidified environment. In our work, [D]-H_6L_9 modified liposome could disrupt more red blood cell membrane under pH 5.0, signifying that it could incite effective endosome/lysosome membrane lysis in endosome/lysosome compartment while remaining quite blood-compatible in systemic circulation (under normal pH of 7.4).

3.3. MTT assay and in vitro cellular apoptosis assay

As could be observed from (Fig. 3A), the MTT assay suggested that the inhibition by D-Lip/Antagomir-10b + PTX and D-Lip/PTX was PTX concentration-dependent. Meanwhile, loading with antagomir-10b did not significantly influence the cytotoxicity on cells, which was consistent with the report that antagomir-10b exerted minimal cytotoxicity on cells [8,11]. The apoptosis assay also suggested similar results (Fig. 3B). The cytotoxicity of PTX-loaded PEG-Lip and D-Lip (loaded with antagomir-10b or not) was similar to each other under all the concentrations selected (Fig. S3), suggesting that D-Lip did not promote cellular delivery of liposomal PTX compared to PEG-Lip under pH 7.4. Paclitaxel at 2 μg/mL was opted for most of the in vitro cellular assay; and distinctive cell viability inhibition rate could be attained under this concentration (49.46 ± 1.12% for D-Lip/Antagomir-10b + PTX and 45.44 ± 12.46% for D-Lip/PTX respectively). It was noteworthy that D-Lip alone did not show any evident inhibition on cell growth

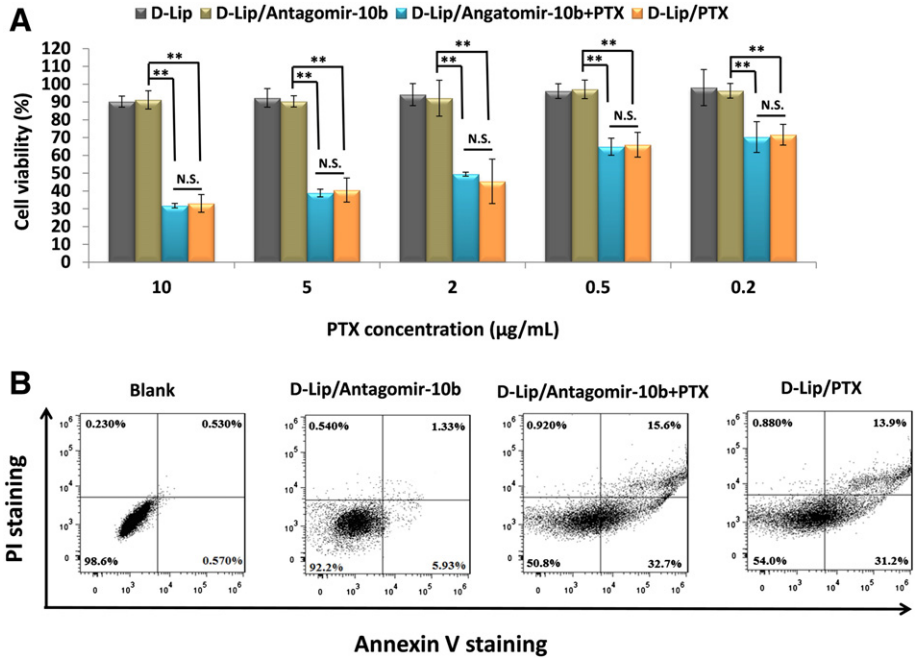

Fig. 3. (A) The cytotoxicity of D-Lip, D-Lip loaded with antagomir-10b (D-Lip/Antagomir-10b), D-Lip loaded with antagomir-10b as well as PTX (D-Lip/Antagomir-10b + PTX) and D-Lip loaded with PTX (D-Lip/PTX). (n = 3, mean ± SD) ** indicated $p < 0.01$, and N.S. indicated there was no significance in difference between each other. (B) The diagrams of the apoptosis assay of D-Lip loaded with paclitaxel and co-delivered with antagomir-10b or not.

(Fig. 3), implying that D-Lip could be deemed as a rather safe agent for antagomirs delivery in this regard.

3.4. Wound healing assay

Wound healing assay could allow the researchers to directly visualize the impact of different formulations on cell migration. D-Lip/Antagomir-10b could hinder the migration of 4 T1 cells as much as Lipofectamine/Antagomir-10b, signifying the potential of D-Lip as a gene vector (Fig. 4). By comparison, it could be clearly observed from the images that compared to all the other groups, D-Lip/Antagomir-10b + PTX exerted the most significant inhibition on cell migration of 4 T1 cells. Although it was reported that free antagomir-10b could also inhibit cellular migration at a much higher concentration (50 μg/mL, about 6.2 μM [11]), the migration inhibition effect of free antagomir-10b under the concentration we applied here (200 nM) was not obvious at all, highlighting the introduction of appropriate gene vectors could enhance the performance of gene delivery. Also, it could be observed from Fig. 4 that both paclitaxel-loaded D-Lip and PEG-Lip could stunt the cellular migration to a similar degree to each other. In fact, *nab*-paclitaxel (albumin-bound 130 nm formulation of paclitaxel) has already been applied to clinical trials for metastatic breast cancer [34], showing that paclitaxel formulation holds great potential in its treatment. Paclitaxel could inhibit cell migration by suppressing microtubule dynamics [35], therefore the co-delivery of paclitaxel and antagomir-10b could impede the migration of metastatic tumor cells further more. Meanwhile, D-Lip/antagomir-10b + PTX showed superior capability in migration hindrance than PEG-Lip/antagomir-10b + PTX. This was perhaps because that D-Lip could deliver antagomir-10b more efficiently compared with PEG-Lip, since the migration inhibition was contributed by the successful delivery of both PTX and antagomir-10b, and both D-Lip/PTX and PEG-Lip/PTX displayed similar inhibition efficiency over cellular migration. This point will be further addressed in the following work.

3.5. Cellular uptake of liposomes and subcellular localization

As shown in Fig. 5A, although not as much as Lipofectamine/Antagomir-10b, the cellular uptake of D-Lip/Antagomir-10b and D-Lip/Antagomir-10b + PTX was close to PEG/Antagomir-10b after 2 h. The cellular uptake of free antagomir-10b was the lowest; which conformed to previous report that without delivery vectors, the cellular uptake of RNA could be quite low [36]. The result could explain in part the rather low migration inhibition efficiency of free antagomir-10b in wound healing assay. The subcellular localization of antagomirs was of great account, for the localization of RNA could have great impact on the transfection outcome [37], and the successful escape of antagomir-10b from endosome/lysosome compartment or the avoidance of endosome/lysosome engulfment would be of utmost importance. According to the results from Fig. 5B, it could be observed that only a small fraction of the fluorescence signal of Cy5-labeled antagomir-10b co-localized with lysosomes. Paclitaxel seemed to exert very little influence on this process (Fig. 5B). Also, it could be concluded from Fig. S4 that the endocytosis of D-Lip was influenced by multiple pathways (with chlorpromazine, amiloride and genistein inhibiting the cellular uptake efficiencies to 72.32 ± 6.23%, 76.23 ± 5.39% and 61.30 ± 3.24% respectively), implying that some of the cellular uptake of D-Lip might have avoided the endosome upon internalization [38,39]. In addition, according to the results of hemolytic assay, in which under pH 5.0 D-Lip caused more hemolysis than pH 7.4, it implied that D-Lip could break the constraint of endosome/lysosome more effectively than PEG-Lip. Nevertheless, the breaking-down of red blood cells (with the hemolysis rate of 16.2 ± 3.2% at 6 h) was not as high as some other reports for gene delivery [18,30,40]. Therefore, it was rational to infer that D-Lip might have avoided the lysosome degradation by at least two mechanisms: one was to avoid the internalization and processing by endosome/lysosome and the other was to escape the endosomes/lysosomes after internalization with the aid of the peptide [D]-H_6L_9. By contrast, PEG-Lip/Antagomir-10b showed almost complete overlay of lysosomes and antagomir-10b, indicating that antagomir-10b could hardly escape

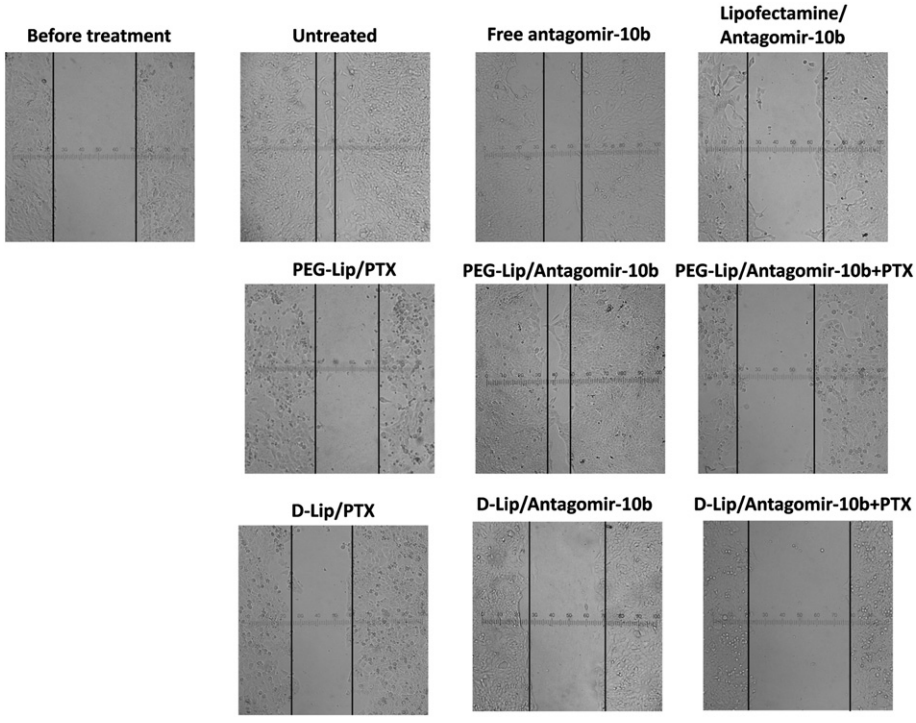

Fig. 4. Representative images showing the inhibition of different preparations on 4 T1 cell migration in wound healing assay. Except for "before treatment", all the other images were taken 48 h after treatment. The dark and straight lines in these pictures designated the rough margins of the 4 T1 cells.

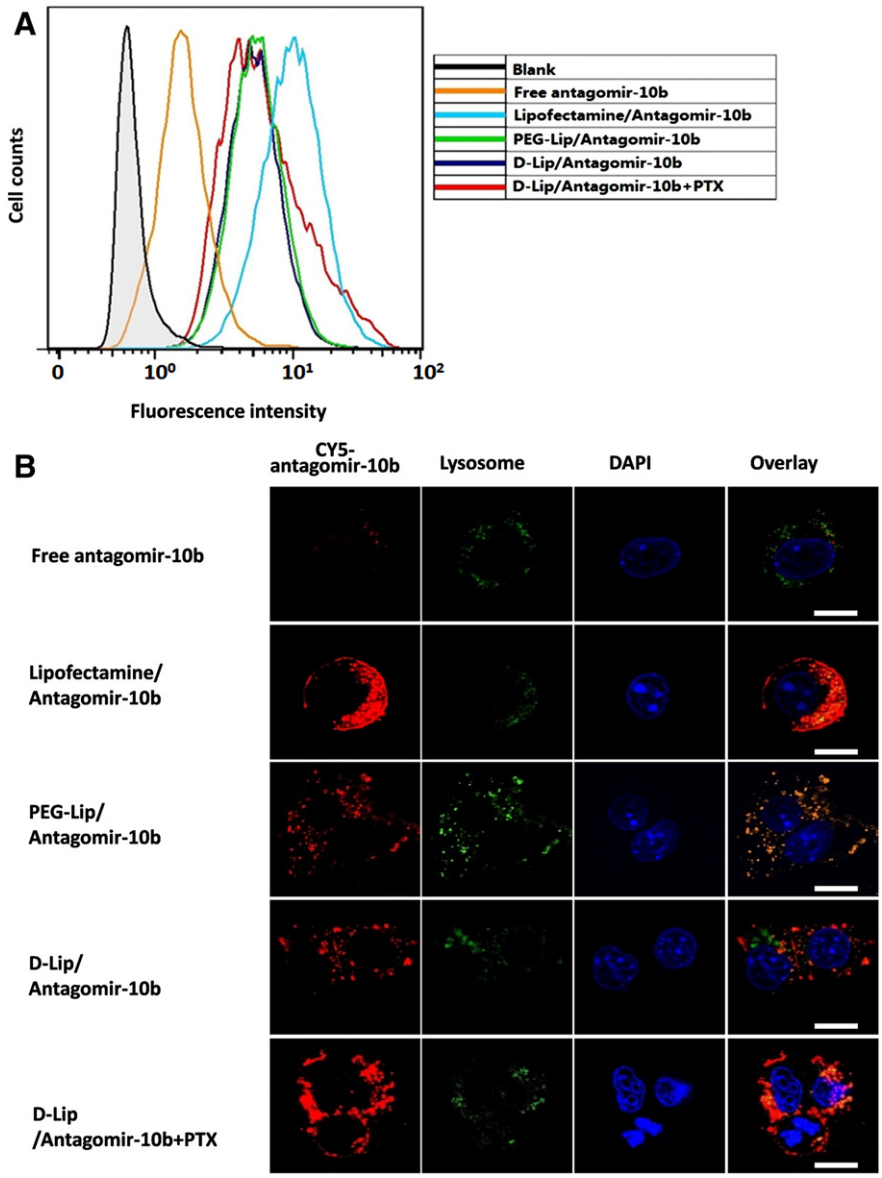

Fig. 5. (A) Cellular uptake of Cy5-labeled antagomir-10b loaded liposomes on 4 T1 cells after 2 h (measured by flow cytometry). (B) Lysosome staining and the intracellular distribution of Cy5-labeled antagomir-10b loaded liposomes on 4 T1 cells after 2 h. Scar bar represents 10 μm. The color yellow in line Overlay denoted the overlay of fluorescence from liposomes (read) and lysosome staining (green). Scale bars represent 10 μm.

from the lysosome, which could negatively influence the gene delivery efficacy.

3.6. In vitro evaluation on the effect of antagomir-10b loaded liposomes on mir-10b silencing and Hoxd10 expression

Mir-10b functioned as metastasis driver thought suppressing the downstream mediator Hoxd10, and was always elevated in metastasis-positive tumor tissues [7,41,42]. Suppression of Hoxd10 could lead to the activation of RhoC, a pro-metastatic gene [7,43]. Therefore the application of antagomir-10b could ultimately lead to the decrease of RhoC and prevent tumor metastasis. The silencing of mir-10b as well as the elevated expression level of Hoxd10 were both regarded as the indexes for the estimation of gene knockdown efficacy of antagomir-10b [7,11]. Through the results in Fig. 6 we can see that both quantitative measurement of RT-PCR on mir-10b and the immunostaining of FITC-conjugated Hoxd10 antibody implied that D-Lip could effectively decrease mir-10b (Fig. 6A) and promote the level of Hoxd10 after loading with antagomir-10b (Fig. 6B). Besides some nucleus abnormity which was mainly caused by its cytotoxicity (Fig. 6B), the delivery of paclitaxel did not significantly influence the expression of Hoxd10 (whether co-delivered with antagomir-10b or not), suggesting that although paclitaxel could obviously inhibit the migration of 4 T1 cells in the wound healing assay, it did not take effect through the suppression of mir-10b; it should be working under a different mechanism, which was directly suppressing microtubule dynamics [35], and impairing cellular motility.

The better gene delivery efficiency of D-Lip was due to the presence of peptide [D]-H_6L_9.The gene delivery capacity of its original peptide [D]-K_6L_9 has already been investigated after stearylation [44]. Although quite effective, only in vitro transfection results have been provided [44] ; as a matter of fact, the strong and indiscriminative cell penetration brought by [D]-K_6L_9 (according to our unpublished results) might render it inapposite for in vivo gene delivery. The cellular permeation of peptide [D]-H_6L_9, on the other hand, was weakened under pH 7.4 compared to [D]-K_6L_9; however, once in the endosomes/lysosomes (pH 5.0), its membrane lytic capacity was incited, inducing remarkable endosome/lysosome membrane destabilization, facilitating the endosome/

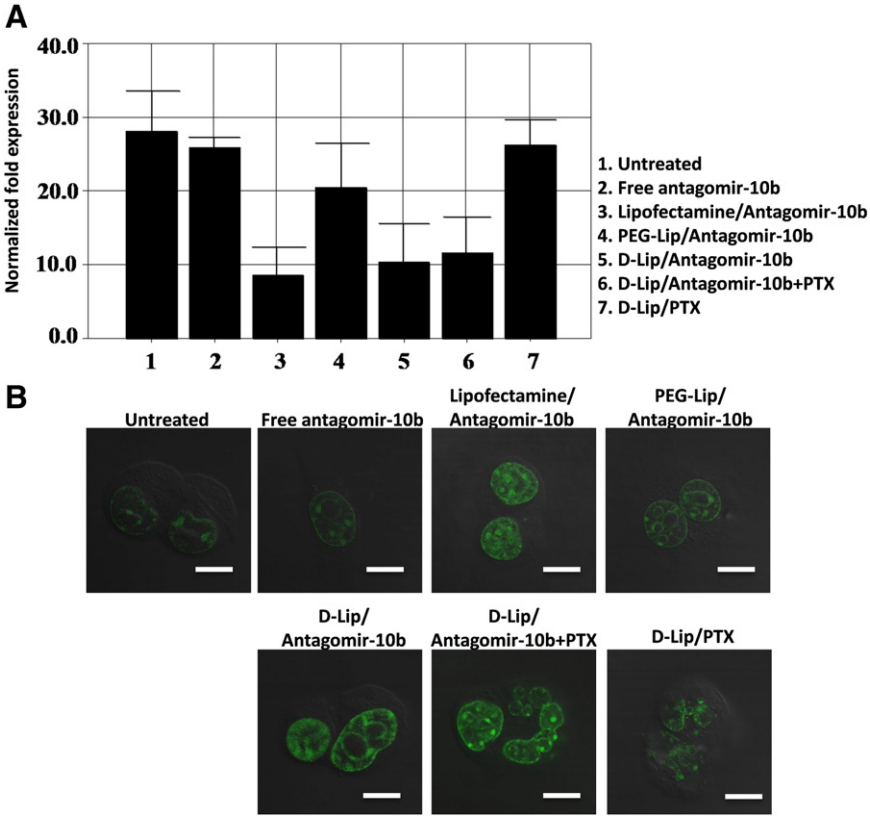

Fig. 6. (A) qRT-PCR measurement of mir-10b in 4 T1 cells after treating with different preparations for 48 h (n = 3, mean ± SD). (B) Representative CLSM images of 4 T1 cells treated with different preparations for 48 h and immunostained with FTIC-conjugated Hoxd10 antibody (green fluorescence). Scale bars represent 10 μm.

lysosome escape of the vesicle it has been attached to and improving gene delivery efficiency. There was also another saying that the hisidine-rich molecules displayed buffering effect upon protonation of the imidazole ring of histidine and could thereby disrupt endosomal membrane by proton sponge effect [45]. So the efficient gene delivery of D-Lip might be attributed to more than just one factor.

3.7. In vivo delivery of antagomir-10b loaded liposomes

As displayed in Fig. 7 (both A and B), 24 h later, PEG-Lip and D-Lip could both achieve efficient accumulation at tumors, showing that the PEGylation was of great significance to the passive tumor accumulation of liposomes, and the decoration of [D]-H_6L_9 did not obviously jeopardize the long circulation effect of PEGylated liposomes. In comparison, free antagomir-10b showed very little retention in almost all the organs, demonstrating that free antagomir-10b might have undergone quick elimination from the systemic circulation. The threshold of glomerular filtration is within the range of 30–50 kDa [46]; since the molecular weight for antagomir-10b was around 8 kDa, it was easy for it to get cleared from systemic circulation through kidney. In the meantime, PEGylated liposomes facilitated the preferential accumulation of liposomes in tumors by EPR effect [47], so the tumor accumulation of antagomir-10b-loaded D-Lip was significantly elevated.

We then evaluated the therapeutic efficacy of different liposomes. In accordance with our in vitro cytotoxic assays, D-Lip and PEG-Lip loaded with PTX successfully delayed the primary tumor development (Fig. 8A). Intriguingly, we found that although both PEG-Lip/PTX and PEG-Lip/antagomir-10b + PTX could inhibit the tumor growth to some extent, D-Lip/PTX and D-Lip/antagomir-10b + PTX could induce more tumor volume reduction when compared with them (Fig. 8A). This might seem eccentric now that D-Lip and PEG-Lip showed very similar in vitro cytotoxicity (Fig. S3). Actually, the peptide D-H_6L_9 that we have chosen in our study was a pH-responsive peptide; according to our unpublished results, D-Lip could be delivered to cells in acidic tumor-mimicking environment (in our set, pH 6.3) more efficiently than cells in normal environment (pH 7.4) in vitro, and its cytotoxicity against cells significantly increased under pH 6.3 compared with pH 7.4, when as for PEG-Lip it remained almost the same. This is due to the histidines in D-H_6L_9 which own a pK_a around 6.5, and its membrane permeation could be potentiated in tumor environment (with acidic pH, which could be as low as 6.0, according to ref. [48]). That is to say, we found that D-H_6L_9 could not only mediate effective endosomal escape but also help deliver more liposomes in acidic environment. Hence, it seemed more and more convincing for us to conclude that the improved therapeutic efficacy of D-Lip/antagomir-10b + PTX in vivo might be owing to both the enhanced delivery of D-Lip's cargo under acidic environment in tumors (as it could be seen from the confocal images of tumor slices in Fig. 5S that the antagomir-10b delivered by D-Lip was greatly increased compared with PEG-Lip) and D-Lip's augmented antagomir-10b delivery efficiency. Although D-Lip and PEG-Lip reached tumors with almost the same efficacy (Fig. 7), their cellular internalization within tumors might be different due to their discrepancy in drug delivery capacity under acidified tumor micro-environment. This phenomenon has been reported in our previous work [24]. As to the better cellular delivery of D-Lip under acidic environment than PEG-Lip, the results we have obtained so far have only been preliminary studies and apparently systematic and massive study should be conducted on the pH-sensitivity of D-Lip in tumor micro-environment in the future. On the other hand, antagomir-10b exerted almost no influence on the growth of primary tumors. Ki67 staining and TUNEL staining of the tumor slices indicated again that among all the groups, only PTX-loaded liposomes could induce more necrosis and apoptosis (Fig. 8E). Body weights increased gradually during the treatment and little difference was observed for different groups, indicating the safety for the in vivo application of different formulations (Fig. 8B). Lung metastasis inhibition of D-Lip/Angatomir-10b + PTX was significantly higher than the rest of

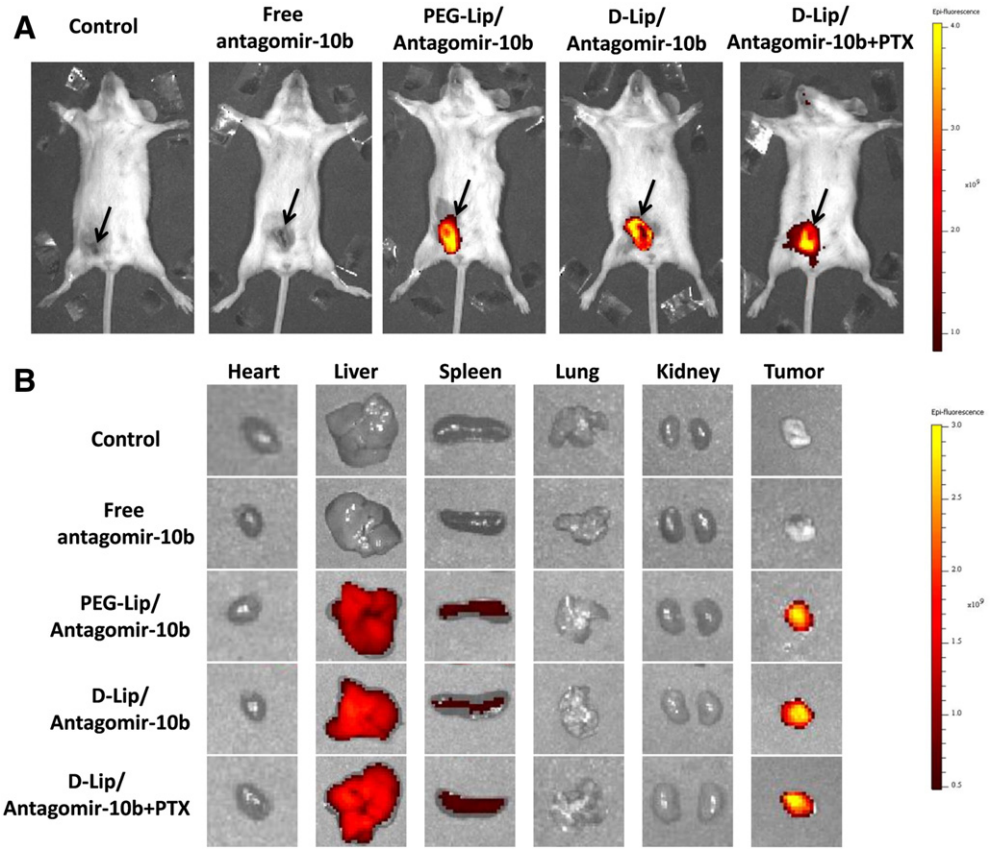

Fig. 7. Representative in vivo (A) and ex vivo (B) images of 4 T1 tumor-bearing BALB/C mice 24 hours after injection of Cy5 labeled antagomir-10b-loaded liposomes. The black arrows in (A) indicated the location of tumors.

other groups (Fig. 8C). It could be inferred from the ELISA assay of Hoxd10 protein that D-Lip exhibited prominent potential in delivering antagomir-10b in vivo (Fig. 8D). By contrast, the lung metastasis inhibition (Fig. 8C) and Hoxd10 up-regulation (Fig. 8D) brought by PEG-Lip/antagomir-10b + PTX were all inferior to D-Lip/antagomir-10b + PTX. It was noteworthy that the dose of antagomir-10b we applied to 4 T1 tumor-bearing mice was only 2 mg/kg, which was distinctively lower than the dose reported before [which was 50 mg/kg, in ref. 11]. Antagomirs were originally considered as efficient and specific silencers of endogenous miRNAs in mice for the loss-of function studies, and was applied usually in the free form [9]. Loading bio-active molecules into nanoparticles could lower the dose required for pharmacological response or to improve the delivery efficiency to certain locations, therefore some antagomir-loaded nano-particulate drug delivery systems have emerged lately [49–52]. Hatakeyama et al. reported that after enveloping antagomir-122 into a multi-functional envelop-type nano devise, the dose for antagomir-122 could be as low as 1 mg/kg, which was much lower than previously required [49]. In our case, the lowered dose for antagomir-10b should be attributed to the altered pharmacokinetic behaviors of PEGylated D-Lip compared to free antagomir-10b, as more antagomir-10b loaded liposomes could be retained within tumors (as shown in Fig. 7) to give play to adequate function in vivo. Thereby it would be cost-efficient to deliver genes in proper vectors.

Endeavors have been attempted for researchers to develop nano-sized carriers delivering anti-microbial peptides (AMPs) for infection therapy or oncotherapy [53–55]. However, not enough attention has been received for AMPs as to their capacity to deliver pharmaceuticals. In fact, AMPs with strong membrane-activity could also be listed among the potential candidates for drug delivery [44,56]. In this work, we have proved that [D]-H_6L_9, one of the synthetic AMPs, could mediate liposomal delivery of antagomir-10b and achieve sufficient gene knockdown of mir-10b (as evidenced by the reduced amount of mir-10b and the increased level of Hoxd10 protein). Co-delivery of PTX could retard the growth of 4 T1 tumors without influencing the up-regulation of Hoxd10 by antagomir-10b.The combination therapy of cancer with drugs and RNA interference has been quite appealing, as the advancement of nanotechnology has made it possible to co-deliver different bio-active therapeutic molecules in a “two-in-one” modality [57–59]. Although antagomir-10b showed remarkable capacity over the inhibition of metastasis (Fig. 8C), it could not control the growth of primary tumors (Fig. 8A) for it does not act in a cytotoxic fashion but instead block the launch of early metastases [11]. Ma suggested that antagomir-10b could be proposed as a prophylactic treatment for tumors that has not yet metastasized [8]. On the other hand, paclitaxel could suppress the growth of primary tumors, but its ability in stifling in vivo metastasis was far from satisfactory. Simultaneous and combined administration of antagomir-10b with paclitaxel by D-Lip could take the advantage and make up for the deficiency of each other. In this sense, D-Lip/Antagomir-10b + PTX could be applied to metastatic breast tumor models of early onset with the inhibitory effect over primary tumor development and metastasis at the same time for a better treatment outcome.

4. Conclusion

In summary, in this study we have devised a liposomal delivery system mediated by an anti-microbial peptide [D]-H_6L_9 (D-Lip), and applied it into the co-delivery of antagomir-10b and PTX. Results suggested that D-Lip loaded with antagomir-10b could efficiently impede the migration of 4 T1 cells in vitro. D-Lip could escape the entrapment of endosomes/lysosomes with the help of the activated [D]-H_6L_9 under acidified environment, therefore resulting in the silencing of mir-10b and up-regulation of Hoxd10 both in vitro and in vivo. Loading D-Lip with PTX could incite strong tumor cell inhibition without

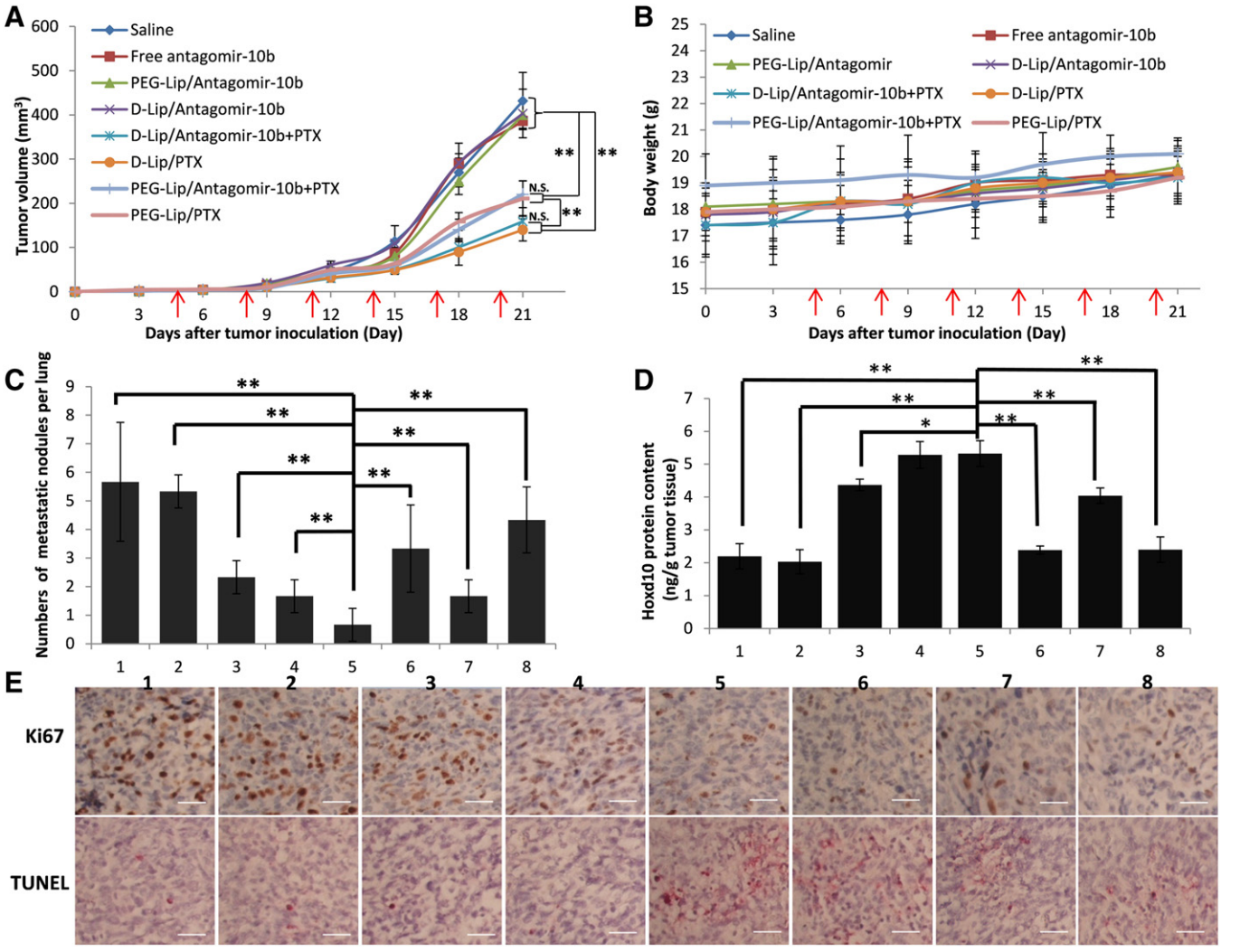

Fig. 8. Therapeutic efficacy evaluation of liposomes on 4 T1 tumor-bearing BALB/C mice. (A)Primary tumor growth curves of mice receiving different preparations (n = 6, mean ± SD). (B) Body weight variations of mice during the treatment (n = 6, mean ± SD). (C) Numbers of metastatic nodules of each lung for different groups (n = 6, mean ± SD). (D) ELISA assay of Hoxd10 protein of tumors at the end of the treatment (n = 3, mean ± SD). (E) Ki67 staining (proliferative cells shown in brown) and TUNEL staining (apoptotic and necrotic cells shown in brownish-red) of tumor tissues. Red arrows in (A) and (B) indicated the days for administration, which were Day 5, 8, 11, 14, 17 and 20. Antagomir-10b was administered at a dose of 2 mg/kg, and PTX was administered at a dose of 2 mg/kg. Bars represented 100 μm. N.S. indicated there was no significance in difference between each other. * and ** indicated $p < 0.05$ and $p < 0.01$ respectively. In (C), (D) and (E), 1 represented group saline, 2 represented group free antagomir-10b, 3 represented group PEG-Lip/Antagomr-10b, 4 represented group D-Lip/Antagomir-10b, 5 represented group D-Lip/Antagomir-10b + PTX, 6 represented group D-Lip/PTX, 7 represented group PEG-Lip/Antagomir-10b + PTX and 8 represented group PEG-Lip/PTX.

influencing the function of antagomir-10b. D-Lip could reach tumors with effect, and for the therapeutic study, co-delivering antagomir-10b with PTX by D-Lid could efficiently inhibit tumor growth and reduce the incidence of lung metastasis. To our knowledge, there has been no report on the [D]-H_6L_9-mediated vehicle delivery so far, and the co-delivery of antagomir-10b with cytotoxic drugs has not yet been investigated to date; we hope that this work could provide researchers with some interesting insights in establishing AMPs-mediated drug delivery systems.

Acknowledgements

The work was funded by the National Basic Research Program of China (973 Program, 2013CB932504) and the National Natural Science Foundation of China (81373337).

Appendix A. Supplementary data

Supplementary data to this article can be found online at http://dx.doi.org/10.1016/j.jconrel.2014.11.010.

References

[1] E. Huntzinger, E. Izaurralde, Gene silencing by microRNAs: contributions of translational repression and mRNA decay, Nature 12 (2011) 99–110.
[2] C.M. Croce, Causes and consequences of microRNA dysregulation in cancer, Nat. Rev. Genet. 10 (2009) 704–714.
[3] J.A. Broderick, P.D. Zamore, MicroRNA therapeutics, Gene Ther. 18 (2011) 1104–1110.
[4] R. Garzon, G. Marcucci, C.M. Croce, Targeting microRNAs in cancer: rationale, strategies and challenges, Nat. Rev. Drug Discov. 9 (2010) 775–789.
[5] D.R. Hurst, M.D. Edmonds, D.R. Welch, Metastamir: the field of metastasis-regulatory microRNA is spreading, Cancer Res. 69 (2009) 7495–7498.
[6] N. Pencheva, S.F. Tavazoie, Control of metastatic progression by microRNA regulatory networks, Nat. Cell Biol. 15 (2013) 546–554.
[7] L. Ma, J. Teruya-Feldstein, R.A. Weinberg, Tumour invasion and metastasis initiated by microRNA-10b in breast cancer, Nature 449 (2007) 682–688.
[8] L. Ma, Role of miR-10b in breast cancer metastasis, Breast Cancer Res. 12 (2010) 210.
[9] J. Krutzfeldt, N. Rajewsky, R. Braich, K.G. Rajeev, T. Tuschl, M. Manoharan, M. Stoffel, Silencing of microRNAs in vivo with 'antagomirs', Nature 438 (2005) 685–689.
[10] K.A. Lennox, R. Owczarzy, D.M. Thomas, J.A. Walder, M.A. Behlke, Improved performance of anti-miRNA oligonucleotides using a novel non-nucleotide modifier, Mol. Ther. Nucleic Acids 2 (2013) e117.
[11] L. Ma, F. Reinhardt, E. Pan, J. Soutschek, B. Bhat, E.G. Marcusson, J. Teruya-Feldstein, G.W. Bell, R.A. Weinberg, Therapeutic silencing of miR-10b inhibits metastasis in a mouse mammary tumor model, Nat. Biotechnol. 28 (2010) 341–347.

[12] T.M. Allen, P.R. Cullis, Liposomal drug delivery systems: From concept to clinical applications, Adv. Drug Deliv. Rev. 65 (2013) 36–48.
[13] Z.Z. Yang, J.Q. Li, Z.Z. Wang, D.W. Dong, X.R. Qi, Tumor-targeting dual peptides-modified cationic liposomes for delivery of siRNA and docetaxel to gliomas, Biomaterials 35 (2014) 5226–5239.
[14] Y. Yan, M. Bjornmalm, F. Caruso, Particle carriers for combating multidrug-resistant cancer, ACS Nano 7 (2013) 9512–9517.
[15] K. Nakamura, A.S. Abu Lila, M. Matsunaga, Y. Doi, T. Ishida, H. Kiwada, A double-modulation strategy in cancer treatment with a chemotherapeutic agent and siRNA, Mol. Ther. 19 (2011) 2040–2047.
[16] H. Yin, E.S. Lee, D. Kim, K.H. Lee, K.T. Oh, Y.H. Bae, Physicochemical characteristics of pH-sensitive poly(L-histidine)-b-poly(ethylene glycol)/poly(L-lactide)-b-poly(-ethylene glycol) mixed micelles, J. Control. Release 126 (2008) 130–138.
[17] H. Wu, L. Zhu, V.P. Torchilin, pH-sensitive poly(histidine)-PEG/DSPE-PEG co-polymer micelles for cytosolic drug delivery, Biomaterials 34 (2013) 1213–1222.
[18] Y. Sato, H. Hatakeyama, Y. Sakurai, M. Hyodo, H. Akita, H. Harashima, A pH-sensitive cationic lipid facilitates the delivery of liposomal siRNA and gene silencing activity *in vitro* and *in vivo*, J. Control. Release 163 (2012) 267–276.
[19] N. Toriyabe, Y. Hayashi, H. Harashima, The transfection activity of R8-modified nanoparticles and siRNA condensation using pH sensitive stearylated-octahistidine, Biomaterials 34 (2013) 1337–1343.
[20] L. Tian, Y.H. Bae, Cancer nanomedicines targeting tumor extracellular pH, Colloids Surf. B: Biointerfaces 99 (2012) 116–126.
[21] T. Jiang, Z. Zhang, Y. Zhang, H. Lv, J. Zhou, C. Li, L. Hou, Q. Zhang, Dual-functional liposomes based on pH-responsive cell-penetrating peptide and hyaluronic acid for tumor-targeted anticancer drug delivery, Biomaterials 33 (2012) 9246–9258.
[22] B.X. Zhao, Y. Zhao, Y. Huang, L.M. Luo, P. Song, X. Wang, S. Chen, K.F. Yu, X. Zhang, Q. Zhang, The efficiency of tumor-specific pH-responsive peptide-modified polymeric micelles containing paclitaxel, Biomaterials 33 (2012) 2508–2520.
[23] W. Zhang, J. Song, B. Zhang, L. Liu, K. Wang, R. Wang, Design of acid-activated cell penetrating peptide for delivery of active molecules into cancer cells, Bioconjug. Chem. 22 (2011) 1410–1415.
[24] Q. Zhang, J. Tang, L. Fu, R. Ran, Y. Liu, M. Yuan, Q. He, A pH-responsive α-helical cell penetrating peptide-mediated liposomal delivery system, Biomaterials 34 (2013) 7980–7993.
[25] Z. Tu, M. Volk, K. Shah, K. Clerkin, J.F. Liang, Constructing bioactive peptides with pH-dependent activities, Peptides 30 (2009) 1523–1528.
[26] L. Li, J. He, R. Eckert, D. Yarbrough, R. Lux, M. Anderson, W. Shi, Design and characterization of an acid-activated antimicrobial peptide, Chem. Biol. Drug Des. 75 (2010) 127–132.
[27] A. Makovitzki, A. Fink, Y. Shai, Suppression of human solid tumor growth in mice by intratumor and systemic inoculation of histidine-rich and pH-dependent host defense–like lytic peptides, Cancer Res. 69 (2009) 3458–3463.
[28] K. Splith, I. Neundorf, Antimicrobial peptides with cell-penetrating peptide properties and vice versa, Eur. Biophys. J. 40 (2011) 387–397.
[29] J. Zhang, L. Miao, S. Guo, Y. Zhang, L. Zhang, A. Satterlee, W.Y. Kim, L. Huang, Synergistic anti-tumor effects of combined gemcitabine and cisplatin nanoparticles in a stroma-rich bladder carcinoma model, J. Control. Release 182 (2014) 90–96.
[30] S.F. Ye, M.M. Tian, T.X. Wang, L. Ren, D. Wang, L.H. Shen, T. Shang, Synergistic effects of cell-penetrating peptide Tat and fusogenic peptide HA2-enhanced cellular internalization and gene transduction of organosilica nanoparticles, Nanomedicine 8 (2012) 833–841.
[31] R. Mo, Q. Sun, J. Xue, N. Li, W. Li, C. Zhang, Q. Ping, Multistage pH-responsive liposomes for mitochondrial targeting anticancer drug delivery, Adv. Mater. 24 (2012) 3659–3665.
[32] N. Papo, A. Braunstein, Z. Eshhar, Y. Shai, Suppression of human prostate tumor growth in mice by a cytolytic D-, L-amino acid peptide: membrane lysis, increased necrosis, and inhibition of prostate- specific antigen secretion, Cancer Res. 64 (2004) 5779–5786.
[33] N. Papo, D. Seger, A. Makovitzki, V. Kalchenko, Z. Eshhar, H. Degani, Y. Shai, Inhibition of tumor growth and elimination of multiple metastases in human prostate and breast xenografts by systemic inoculation of a host defense-like lytic peptide, Cancer Res. 66 (2006) 5371–5378.
[34] W.J. Gradishar, D. Krasnojon, S. Cheporov, A.N. Makhson, G.M. Manikhas, A. Clawson, P. Bhar, J.R. McGuire, J. Iglesias, Phase II trial of *nab*-paclitaxel compared with docetaxel as first-line chemotherapy in patients with metastatic breast cancer: final analysis of overall survival, Clin. Breast Cancer 12 (2012) 313–321.
[35] A. Ganguly, H. Yang, F. Cabral, Class III β-tubulin counteracts the ability of paclitaxel to inhibit cell migration, Oncotarget 2 (2011) 368–377.
[36] Y.L. Chiu, A. Ali, C.Y. Chu, H. Cao, T.M. Rana, Visualizing a correlation between siRNA localization, cellular uptake, and RNAi in living cells, Chem. Biol. 11 (2004) 1165–1175.
[37] J. Gilleron, W. Querbes, A. Zeigerer, A. Borodovsky, G. Marsico, U. Schubert, K. Manygoats, S. Seifert, C. Andree, M. Stoter, H. Epstein-Barash, L. Zhang, V. Koteliansky, K. Fitzgerald, E. Fava, M. Bickle, Y. Kalaidzidis, A. Akinc, M. Maier, M. Zerial, Image-based analysis of lipid nanoparticle–mediated siRNA delivery, intracellular trafficking and endosomal escape, Nat. Biotechnol. 31 (2013) 638–646.
[38] S. Xiang, H. Tong, Q. Shi, J.C. Fernandes, T. Jin, K. Dai, X. Zhang, Uptake mechanisms of non-viral gene delivery, J. Control. Release 158 (2012) 371–378.
[39] S. Xu, B.Z. Olenyuk, C.T. Okamato, S.F. Hamm-Alvarez, Targeting receptor-mediated endocytotic pathways with nanoparticles: rationale and advances, Adv. Drug Deliv. Rev. 65 (2013) 121–138.
[40] S. Li, Z. Su, M. Sun, Y. Xiao, F. Cao, A. Huang, H. Li, Q. Ping, C. Zhang, An arginine derivative contained nanostructure lipid carriers with pH-sensitive membranolytic capability for lysosomolytic anti-cancer drug delivery, Int. J. Pharm. 436 (2012) 248–257.
[41] L. Ma, J. Young, H. Prabhala, E. Pan, P. Mestdagh, D. Muth, J. Teruya-Feldstein, F. Reinhardt, T.T. Onder, S. Valastyan, F. Westermann, F. Speleman, J. Vandesompele, R.A. Weinberg, miR-9, a MYC/MYCN-activated microRNA, regulates E-cadherin and cancer metastasis, Nat. Cell Biol. 12 (2010) 247–256.
[42] A. Schuldt, Micromanaging metastasis, Nat. Cell Biol. 9 (2007) 1121.
[43] M. Negrini, G.A. Calin, Breast cancer metastasis: a microRNA story, Breast Cancer Res. 10 (2008) 203.
[44] W. Zhang, J. Song, R. Liang, X. Zheng, J. Chen, G. Li, B. Zhang, K. Wang, X. Yan, R. Wang, Stearylated antimicrobial peptide [D]-K6L9 with cell penetrating property for efficient gene transfer, Peptides 46 (2013) 33–39.
[45] A.K. Varkouhi, M. Scholte, G. Storm, H.J. Haisma, Endosomal escape pathways for delivery of biological, J. Control. Release 151 (2011) 220–228.
[46] A. Ruggiero, C.H. Villa, E. Bander, D.A. Rey, M. Bergkvist, C.A. Batt, K. Manova-Todorova, W.M. Deen, D.A. Scheinberg, M.R. McDevitt, Paradoxical glomerular filtration of carbon nanotubes, Proc. Natl. Acad. Sci. U. S. A. 107 (2010) 12369–12374.
[47] N. Bertrand, J. Wu, X. Xu, N. Kamaly, O.C. Farokhzad, Cancer nanotechnology: the impact of passive and active targeting in the era of modern cancer biology, Adv. Drug Deliv. Rev. 66 (2014) 2–25.
[48] D. Neri, C.T. Supuran, Interfering with pH regulation in tumours as a therapeutic strategy, Nat. Rev. Drug Discov. 10 (2011) 767–777.
[49] H. Hatakeyama, M. Murata, Y. Sato, M. Takahashi, N. Minakawa, A. Matsuda, H. Harashima, The systemic administration of an anti-miRNA oligonucleotide encapsulated pH-sensitive liposome results in reduced level of hepatic microRNA-122 in mice, J. Control. Release 173 (2014) 43–50.
[50] M. Zhang, X. Zhou, B. Wang, B.C. Yung, L.J. Lee, K. Ghoshal, R.J. Lee, Lactosylated gramicidin-based lipid nanoparticles (Lac-GLN) for targeted delivery of anti-miR-155 to hepatocellular carcinoma, J. Control. Release 168 (2013) 251–261.
[51] M. Takahashi, N. Yamada, H. Hatakeyama, M. Murata, Y. Sato, N. Minakawa, H. Harashima, A. Matsuda, In vitro optimization of 20-OMe-40-thioribonucleoside–modified anti-microRNA oligonucleotides and its targeting delivery to mouse liver using a liposomal nanoparticle, Nucleic Acids Res. 41 (2013) 10659–10667.
[52] X.Q. Liu, W.J. Song, T.M. Sun, P.Z. Zhang, J. Wang, Targeted delivery of antisense inhibitor of miRNA for antiangiogenesis therapy using cRGD-functionalized nanoparticles, Mol. Pharm. 8 (2011) 250–259.
[53] P. Urban, J.J. Valle-Delgado, E. Moles, J. Margues, C. Diez, X. Fernandez-Busquets, Nanotools for the delivery of antimicrobial peptides, Curr. Drug Targets 13 (2012) 1158–1172.
[54] C. Huang, H. Jin, Y. Qian, S. Qi, H. Luo, Q. Luo, Z. Zhang, Hybrid melittin cytolytic peptide-driven ultrasmall lipid nanoparticles block melanoma growth in vivo, ACS Nano 7 (2013) 5791–5800.
[55] C. Lopez-Abarrategui, V. Figueroa-Espi, O. Reyes-Acosta, E. Reguera, A.J. Otero-Gonzalez, Magnetic nanoparticles: new players in antimicrobial peptide therapeutics, Curr. Protein Pept. Sci. 14 (2013) 595–606.
[56] K.K. Hou, H. Pan, G.M. Lanza, S.A. Wickline, Melittin derived peptides for nanoparticle based siRNA transfection, Biomaterials 34 (2013) 3110–3119.
[57] T.M. Sun, J.Z. Du, Y.D. Yao, C.Q. Mao, S. Dou, S.Y. Huang, P.Z. Zhang, K.W. Leong, E.W. Song, J. Wang, Simultaneous delivery of siRNA and paclitaxel via a "two-in-one" micelleplex promotes synergistic tumor suppression, ACS Nano 5 (2011) 1483–1494.
[58] A. Eldar-Boock, D. Polyak, A. Scomparin, R. Satchi-Fainaro, Nano-sized polymers and liposomes designed to deliver combination therapy for cancer, Curr. Opin. Biotechnol. 24 (2013) 682–689.
[59] O. Taratula, A. Kuzmov, M. Shah, O.B. Garbuzenko, T. Minko, Nanostructured lipid carriers as multifunctional nanomedicine platform for pulmonary co-delivery of anticancer drugs and siRNA, J. Control. Release 171 (2013) 349–357.